

02 Temperature-sensitive fluorescence decay kinetics of thioflavin T derivatives in glycerol

© V.I. Stsiapura

Yanka Kupala Grodno State University,
230023 Grodno, Belarus

e-mail: stsiapura@gmail.com

Received December 22, 2021

Revised February 07, 2022

Accepted February 15, 2022

Possible use of Thioflavin T based fluorescent molecular rotors as temperature sensors was assessed in this work. Fluorescent properties of Thioflavin T and its derivative 6-Me-BTA-2C in 99% glycerol were studied using steady-state and time-resolved fluorescence spectroscopy methods. For Thioflavin T in glycerol it has been found that temperature growth from 261 K to 353 K results in ~ 3 orders of magnitude increase of non-radiative decay rate constant k_{nr} for the excited state of the molecule. Fluorescence decay studies by time-correlated single photon counting method showed that fluorescence decay kinetics of Thioflavin T in glycerol can be used for temperature measurements in the range 260–290 K. For 6-Me-BTA-2C molecule the range of the maximal sensitivity was shifted to higher temperatures (280–320 K). The obtained results about fluorescent properties and decay kinetics of Thioflavin T based dyes in highly viscous media can be used to develop nanoscale temperature sensors.

Keywords: temperature sensor, fluorescent molecular rotor, nanothermometry, thioflavin T, TICT.

DOI: 10.21883/EOS.2022.05.54439.13-22

Temperature is one of the important parameters characterizing the state of thermodynamic systems. For temperature measurements, a large number of thermometers and sensors have been developed, the principle of operation of which is based on the temperature dependence of such physical quantities as volume, electric potential, conductivity, etc. In most thermometers, the size of the sensor elements is in the range from tens of micrometers to millimeters, which does not allow for measuring temperature gradients (e.g. in liquids) with high spatial resolution. Temperature measurement with spatial resolution of the order of nanometers, i.e. nanothermometry [1–5], requires miniaturization of temperature-sensitive elements, which can be achieved by using fluorescent/luminescent molecules or nanoparticles with temperature-sensitive luminescence as temperature sensors. It is important to note that sensors of this kind allow for non-contact measurements, are characterized by a fast response time, the ability to obtain data with high spatial resolution characteristic of optical microscopy, are biocompatible and can be used in biological research [3]. Numerous temperature sensors based on organic dyes [6,7], fluorescent proteins, semiconductor quantum dots, nanoparticles doped with dyes or lanthanide ions, etc., are discussed in detail in recent reviews [1,8].

Recently, considerable interest has been paid to development of temperature sensors based on fluorescent molecular rotors (FMR). Molecules belonging to the FMR class are characterized by significant structural-conformational changes in the excited state, which manifests itself in significant dependence of the fluorescence intensity on temperature and viscosity of the microenvironment [9–

11]. Such behavior is characteristic of thioflavin T [12–14], diphenylmethane (for example, auramine O [15–17]) and triphenylmethane [18,19] dyes, [p-(dialkylamino) benzyldene] malononitrile [20,21], a series of probes based on BODIPY [22–24]. In this regard, a number of new molecular rotors based on BODIPY [22,24], porphyrin dimers [25], and polymers with a stilbene-like chromophore group are tested as thermosensitive sensor molecules [26].

Previously, in a series of articles [13,14,27,28], it was shown that the thioflavin T (ThT) benzothiazole-aniline dye (Fig. 1) belongs to the FMR class, and the quantum yield of its fluorescence is determined mainly by viscosity or the rigidity of the microenvironment. On the basis of quantum chemical calculations [12,14,29,30] a model of photophysical properties of ThT was proposed, where it is suggested that intramolecular charge transfer (TICT) occurs during photoexcitation, accompanied by a change in the dihedral angle between the aromatic fragments of the molecule from $\varphi \sim 37$ to 90° , leading to formation of a non-fluorescent TICT state. This model was confirmed using femtosecond absorption spectroscopy [14,31]: experimental evidence of photoinduced intramolecular charge transfer

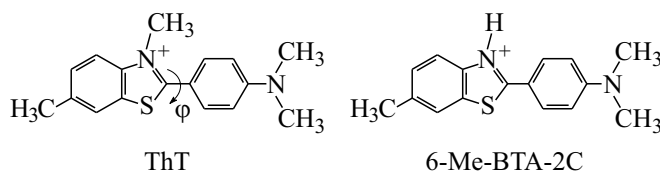


Figure 1. Structural diagrams of benzothiazol-aniline dyes exhibiting FMR properties.

resulting in formation of the intermediate nonfluorescent TICT state was obtained and it was shown that nonequilibrium locally excited (LE) state of ThT is responsible for fluorescence emission.

The rate of the TICT process leading to nonradiative deactivation of the ThT excited state strongly depends on temperature and viscosity of the microenvironment, which makes it possible to estimate temperature of the medium, where the molecular rotor is located, based on measurements of the intensity or fluorescence decay kinetics.

From a practical point of view, in addition to fluorescence parameter sensitivity to temperature, for a sensor molecule it is also important to select a solvent whose viscosity would provide a high quantum yield of FMR fluorescence in the required temperature range. For the FMRs based on benzothiazole-aniline dyes considered in this study (Fig. 1), a significant fluorescence quantum yield is observed at viscosities of $\eta \sim 1000 \text{ mPa} \cdot \text{s}$, therefore glycerol was selected as a solvent in this article.

The aim of this article was to study the effect of temperature on the quantum yield and fluorescence kinetics of benzothiazole-aniline derivatives of ThT and to evaluate the possibility of using these dyes as fluorescent sensors for nanothermometry.

Experimental procedure

Samples of 2-[4'-(dimethylamino)phenyl]-6-methylbenzothiazole (6-Me-BTA-2) with a purity of 99% and thioflavin T (ThT) with a purity of > 95% were purchased from Anaspec (USA) and used without additional purification (Fig. 1). Solutions were prepared using glycerol with a purity of $\geq 99.5\%$ (G9012, Sigma). Conversion of neutral 6-Me-BTA-2 molecules into the protonated cationic form 6-Me-BTA-2C was carried out by adding a small amount of concentrated acid HCl (less than 1% by volume).

Electronic absorption spectra were obtained using a SPECORD-200 PC double-beam spectrophotometer (Analytik Jena, Germany). Registration of stationary fluorescence spectra was carried out using a SM2203 spectrofluorimeter (Solar, Belarus). Fluorescence spectra and kinetics were measured as a function of temperature in a thermostatically controlled cell compartment (range 293–323 K) or in a Dewar flask equipped with heating and cooling elements. The temperature was controlled with HI 93530 electronic thermometer (Hanna Instruments). Measurements of fluorescence quantum yields Φ for ThT and 6-Me-BTA-2C in glycerol at 323 K were carried out by the relative method [32] using ThT solution in 1-butanol as a standard with $\Phi = 0.0043$ at temperature of 298 K [14,27]. Values Φ for glycerol solutions at temperatures other than 323 K were calculated by comparing the integral intensities of dye luminescence. In this case, changes in the refractive index of the medium and the absorption spectra of ThT and 6-Me-BTA-2C with temperature were neglected.

Data on the refractive index and viscosity of glycerol for temperatures above 293 K were taken from the reference book [33]. For the temperature range of 193–293 K, viscosity of glycerol was estimated by the formula

$$\eta = \eta^0 \exp\left(\frac{A}{T^3} + BT + \frac{C}{T}\right) \quad (1)$$

with parameters $\ln(\eta^0/\text{mPa}\cdot\text{s})=25.8709$, $A=3.0942 \cdot 10^8 \text{ K}^3$, $B = -0.0327 \text{ K}^{-1}$ and $C = -6291.03 \text{ K}$ (see equation (7) from the article [34]).

Fluorescence decay lifetime was measured on a pulsed fluorimeter [35] using the time-correlated single photon counting (TCSPC) method [36]. Fluorescence was excited using LDH-405 pulsed laser diode (Picoquant, Germany) with wavelength of 407 nm, a duration of 70 ps, and pulse repetition rate of 10 MHz. The recording system included a PMA-182 photodetector unit, as well as a TimeHarp 200 device for time-correlated single photon counting (PicoQuant, Germany). The time resolution of the pulse fluorimeter is 60 ps [35]. Analysis of the decay kinetics taking into account the duration of the instrumental function of the spectrometer *IRF* was performed using the software described earlier [35,37]. The fluorescence decay law $F(t)$ was represented by a set of exponents

$$F(t) = \sum_j \alpha_j \exp(-t/\tau_j), \quad (2)$$

where α_j, τ_j — amplitude and lifetime of the j th component. The contribution of the j th kinetic component to the luminescence was estimated as $S_j \sim \alpha_j \tau_j$. As a characteristic of the duration of the multiexponential decay kinetics, we used the mean lifetime $\langle \tau \rangle$,

$$\langle \tau \rangle = \frac{\sum \alpha_j \tau_j^2}{\sum \alpha_j \tau_j}. \quad (3)$$

Results and discussion

Dependence of fluorescence quantum yield on temperature

The photophysical properties of ThT-based FMR in low-viscosity solvents are determined by occurrence of intramolecular charge transfer process in the excited state of dye molecules with formation of non-fluorescent TICT state with effective rate constant k_{TICT} , which competes with the process of radiative transition from locally excited LE state with a rate constant k_r . During TICT state formation the benzothiazole and aniline fragments of the considered FMRs have to rotate relative to each other, causing movement of nearby solvent molecules which makes TICT process rate to be dependent on microenvironment viscosity. For the case of low viscosities, the TICT process is the main non-radiative process of deactivation of the excited state [31], so we can assume that for these conditions the

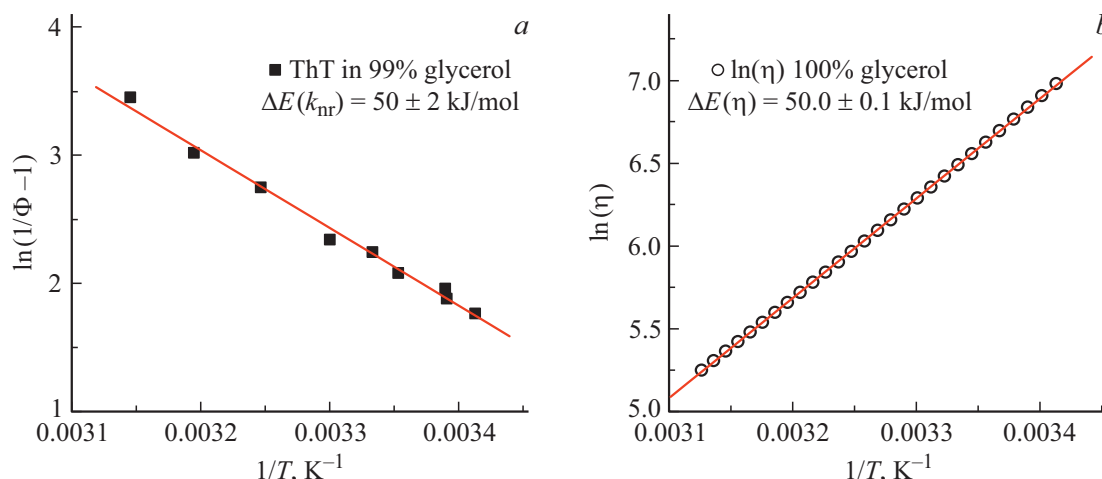


Figure 2. Arrhenius plots $\ln(1/\Phi-1)$ for ThT in 99%-glycerol (a) and the logarithm of glycerol viscosity (b) on the reciprocal temperature in the temperature range of 293–320 K.

total rate constant of non-radiative processes will be equal to

$$k_{nr} \approx k_{\text{TICT}} = k_0 \exp(-\Delta E(k_{nr})/RT), \quad (4)$$

where R — universal gas constant, T — temperature. Here, the TICT process is considered to be thermally activated with activation energy $\Delta E(k_{nr})$, and its rate is affected by both temperature and viscosity properties of the microenvironment. The activation energy of the TICT process will be contributed by both energy barrier ΔE_{int} on the reaction pathway of TICT state formation for the isolated FMR molecule, and the activation energy of the viscous flow of the solvent $\Delta E(\eta)$ (due to the need to move the solvent molecules during the rotation of the FMR fragments). Based on the measurement of the fluorescence quantum yield Φ , one can determine the ratio of the rate constants $k_{nr}/k_r = 1/\Phi - 1$ and obtain the activation energy $\Delta E(k_{nr})$. For ThT and 6-Me-BTA-2C the quantum yields in 99% glycerol at 323 K were measured by the relative method [32], the obtained values were $\Phi = (26 \pm 3) \cdot 10^{-3}$ and $(20 \pm 2) \cdot 10^{-2}$ respectively. The values of the quantum yield at other temperatures were calculated by comparing the integrated dye luminescence intensities.

Figure 2, a shows the dependence of $\ln(k_{nr}/k_r)$ for ThT in 99%-glycerol on the reciprocal temperature $1/T$ for the range $T = 293\text{--}320$ K, and the activation energy $\Delta E(k_{nr}) = 50 \pm 2$ kJ/mol is determined. The value of $\Delta E(k_{nr})$ coincides in value with the activation energy of the viscous flow of glycerol $1/\eta = 1/\eta_0 \exp(-\Delta E(\eta)/RT)$ with $\Delta E(\eta) = (50.0 \pm 0.1)$ kJ/mol (Fig. 2, b) in the given temperature range. Coincidence of the values of $\Delta E(k_{nr})$ and $\Delta E(\eta)$ indicates the practical absence of the energy barrier ΔE_{int} on the path of the charge transfer reaction for ThT (i.e. a barrier-free reaction is implemented for an „isolated“ dye molecule), and the activation energy of the non-radiative process is determined by the temperature dependence of the viscosity properties of the solvent.

At temperatures below 293 K, the glycerol solution passes into the amorphous glass phase [34] (the melting point of glycerol is $T_m \sim 291$ K, and the glass transition temperature is $T_g \sim 193$ K), and its viscosity does not obey the Arrhenius dependence. To calculate viscosities of glycerol at temperatures of $T < 293$ K, formula (1) was used, and Fig. 3, a shows the dependence $1/\eta$ for pure glycerol on the reciprocal temperature.

The dependence of the ratio of the rate constants k_{nr}/k_r on $1/T$ on a semilogarithmic scale for the temperature range of 261–353 K is non-linear, which indicates a change in the effective activation energy $\Delta E(k_{nr})$ for non-radiative rate constant k_{nr} as a function of temperature (from $\Delta E(k_{nr}) \sim 25$ kJ/mol to 83 kJ/mol), and $\Delta E(k_{nr})$ decreases with increasing temperature. A decrease in temperature leads to an increase in viscosity of the glycerol solution and a significant decrease in the rate constant k_{TICT} , therefore, starting from a certain moment, the assumption of the dominant contribution of k_{TICT} to the total rate constant k_{nr} of non-radiative deactivation (4) for ThT may cease to be performed. However, as can be seen in Fig. 3, a, there is a good correlation between the k_{nr}/k_r and $1/\eta$ dependences on the reciprocal temperature, and there are no indications of the contribution of additional channels of non-radiative deactivation at low temperatures and high viscosities region. Moreover, the decrease in the ratio k_{nr}/k_r occurs faster than for the quantity $1/\eta$, which may indicate an increase in the rate constant of the radiative transition k_r with an increase in $1/T$ (the quantity k_r depends on the refractive index of the medium [38,39], the value of which increases with decreasing temperature [40]). Thus, approximation (4) about the dominant contribution of k_{TICT} to the total rate constant of non-radiative deactivation k_{nr} of the excited state of ThT is valid for glycerol solutions up to temperatures of $T \sim 260$ K, and there is a correlation of k_{nr} with the reciprocal of the medium viscosity $1/\eta$.

It is important to distinguish the concept of viscosity η , which is a macroscopic parameter characterizing the ensemble-averaged value of intermolecular interactions of solvent molecules with each other (in this case, for glycerol), from microviscosity η_m , which describes the frictional effect of the solvate shell on the diffusion-controlled process of mutual rotation of ThT molecular fragments during the TICT reaction. The ThT fluorescence intensity provides information on the microviscosity η_m of the dye immediate environment. Depending on the energy of intermolecular interactions of solvent molecules with each other and with a dye molecule, the value of microviscosity may differ in magnitude from the macroscopic viscosity parameter. An additional complication is that the size of the ThT molecular fragments undergoing rotation is comparable to the size of the solvent molecules. In this regard, the solvent cannot be considered as a homogeneous medium, and the configuration of the molecules included in the solvation shell will form a certain „cavity“ with a ThT molecule enclosed inside, and the shape and volume of such „cavity“ will fluctuate in time due to the participation of molecules of the solvate shell in thermal motion. If the characteristic time required to change the volume/shape of such a „cavity“ due to intermolecular collisions is much shorter than the lifetime of the excited LE state of ThT, then the microenvironment of various dye molecules can be considered approximately uniform due to dynamic averaging. Otherwise, it is necessary to take into account the heterogeneity of the ThT microenvironment associated with the difference in the configuration of the solvent molecules surrounding the solvate. This situation can be implemented for glycerol solutions, which at temperatures below 293 K, passes into the amorphous glass phase, which is accompanied by a significant increase in viscosity and inhibition of inter- and intramolecular motions. As temperature decreases, heterogeneity of the microenvironment parameters at the localization areas of dye molecules will increase, while the mobility of the solvate shell will decrease, as in the case of introduction of ThT molecules into rigid matrices.

It can be expected that the heterogeneity in the microenvironment of ThT molecules will affect dynamics of TICT process, leading to non-monoexponential fluorescence decay kinetics (see below). Nevertheless, it is interesting to note that the value k_{nr} estimated based on the fluorescence quantum yield, which characterizes the microviscosity of the dye environment η_m (more precisely, its value averaged over the ensemble of ThT molecules), correlates well with the reciprocal of the macroscopic viscosity parameter η for glycerol (Fig. 3, *a*).

Thus, for the temperature range of 261–285 K, the effective activation energy of the non-radiative transition in 99%-glycerol is $\Delta E(k_{nr}) = 74 \pm 2$ kJ/mol, which practically corresponds to the value $\Delta E(\eta) = 71.8 \pm 0.6$ kJ/mol calculated based on the viscosity data for 100%-glycerol.

Changing the temperature in the range $T = 260$ – 350 K can change the value of the rate constant k_{nr} of the non-radiative transition (more precisely, the ratio k_{nr}/k_r) for ThT

Table 1. Parameters of ThT fluorescence decay kinetics in 99%-glycerol at 480 nm for various temperatures, $\lambda_{exc} = 407$ nm

<i>T</i> , K	α_1	τ_1 , ns	S_1 , %	α_2	τ_2 , ns	S_2 , %	$\langle\tau\rangle$, ns	χ^2
248	1	2.24	100.0				2.24	1.24
	0.965	2.17	94.1	0.035	3.76	5.9	2.26	1.14
263	1	1.86	100.0				1.86	2.19
	0.312	1.09	19.3	0.688	2.06	80.7	1.87	1.11
278	1	1.04	100.0				1.04	8.52
	0.538	0.53	32.2	0.462	1.29	67.8	1.05	1.13
283	1	0.77	100.0				0.77	8.46
	0.635	0.42	41.3	0.365	1.04	58.7	0.79	1.23
288	1	0.58	100.0				0.58	9.21
	0.729	0.34	52.1	0.271	0.85	47.9	0.59	1.30
295	1	0.38	100.0				0.38	8.00
	0.878	0.27	72.2	0.122	0.73	27.8	0.40	1.11

in glycerol by 3 orders of magnitude. The fluorescence quantum yield of ThT in 99% glycerol at 276 K is $\Phi \sim 0.46$ and decreases significantly with increasing temperature.

As for most other FMRs, the lifetime of the excited LE state for ThT in glycerol is comparable to the characteristic times of vibrational and solvent relaxation. As temperature changes, their ratio changes, which manifests itself in a shift and broadening of the steady-state ThT fluorescence spectrum depending on the temperature (Fig. 3, *b*). An increase in temperature from 260 to 323 K leads to a bathochromic shift of the fluorescence spectrum by ~ 10 nm.

Figure 4 shows the fluorescence spectra of the 6-Me-BTA-2C cation in 99% glycerol at various temperatures. As in the case of ThT, a change in temperature affects both the intensity and the position and shape of the fluorescence spectra. An increase in temperature is accompanied by a long-wavelength shift of the spectra (from 474 to 481 nm) and a slight increase in the half-width of the fluorescence band. In the temperature range of 275–343 K, the fluorescence quantum yield of 6-Me-BTA-2C changes by a factor of ~ 12 .

Kinetics of fluorescence decay in glycerol

Fluorescence decay curves for ThT in 99%-glycerol at various temperatures are shown in Fig. 5. The experimental kinetic curves were modeled by a multiexponential decay function (2). The modeling quality was assessed on the basis of the reduced χ^2 criterion, which takes values ~ 1 with a good fit, and the graph of weighted differences (Fig. 5, *d*) between the experimental and calculated decay kinetics curves.

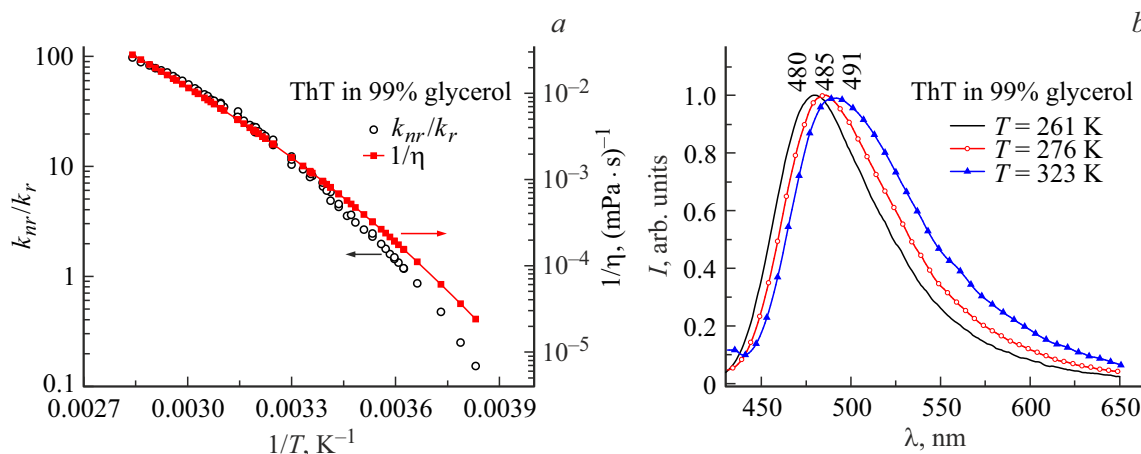


Figure 3. (a) Dependences of $1/\Phi - 1 = k_{nr}/k_r$ for ThT in 99%-glycerol and $1/\eta$ for glycerol on the reciprocal temperature in the range of 260–350 K. (b) Normalized ThT fluorescence spectra in 99%-glycerol at various temperatures. $\lambda_{exc} = 415$ nm.

It was found that the ThT decay kinetics has a non-monoexponential character (Fig. 5, *c, d*), depends on the fluorescence detection wavelength (Fig. 6), and to describe it, it is necessary to use at least 2 or 3 exponential components. The parameters of the fluorescence attenuation kinetics of ThT in glycerol for various temperatures and fluorescence wavelengths are given in Tables 1 and 2.

The reasons for the non-monoexponential fluorescence attenuation kinetics can be both the heterogeneity of the microenvironment of ThT molecules in glycerol and occurrence of spectral relaxation in the excited state of the dye due to solvent repolarization. It is important to note that the rates of solvent relaxation and deactivation of the excited LE state for ThT in glycerol are close in magnitude. For example, the solvate relaxation time in glycerol at 298 K, which is $\tau_S \sim 0.5$ ns [41], practically coincides with the fluorescence lifetime of ThT (τ) = 0.4 ns under the same conditions.

Thus, the shift of the instantaneous fluorescence spectra (time-resolved fluorescence spectra) of the dye to the long wavelength region due to spectral relaxation occurs in the same time range as the decrease in the population of the excited LE state, and this significantly complicates the fluorescence decay kinetics, which is recorded at certain wavelengths. Building of a physical model of the FMR excited state deactivation dynamics for the case of high-viscosity environment is not the aim of this article. In this regard, the description of the decay kinetics was carried out using a multiexponential model, without giving the parameters α_j , τ_j a definite physical meaning. Acceptability of the description of the kinetics was evaluated on the basis of the reduced χ^2 criterion (Tables 1, 2), and the average lifetime (τ) was used to characterize the duration of the multiexponential attenuation kinetics.

In the region of the maximum position of the stationary fluorescence spectrum of ThT at ~ 480 nm, the kinetics can be satisfactorily described using two exponential components (Table 1), and the average lifetime (τ) exhibits a

temperature dependence, changing from ~ 2.2 (at 248 K) to ~ 0.4 ns (at 295 K). However, it should be noted that even at a constant solution temperature, the fluorescence emission wavelength has an important effect on the shape of the attenuation kinetics and the magnitude (τ). For ThT solution at $T \sim 277$ K (Table 2, Fig. 6, *a*) the value (τ) increases by ~ 2 times with increasing detection wavelength from 430 to 680 nm, and to describe the kinetics at the short-wavelength and long-wavelength edges of the spectrum, the introduction of an additional short-lived component is required. Moreover, at the red edge of the spectrum, this short-lived component has a negative amplitude (Table 2), indicating that at the given wavelengths, at the initial stage, there is some increase in the fluorescence signal and only then decay. The presence of an additional short-lived component indicates occurrence of a process of spectral relaxation leading to acceleration of fluorescence decay at the short-wavelength edge and slowdown in decay at the long-wavelength edge of the spectrum.

Comparison of data on the quantum yield and fluorescence kinetics of ThT in glycerol (Fig. 5) makes it possible to determine the radiative transition constant from the excited LE state in 99%-glycerol $k_r \approx 0.4 \cdot 10^9$ s $^{-1}$ with a relative error of 10% (assuming that the fluorescence decay time at 480 nm corresponds to the lifetime of the LE state).

The duration of fluorescence kinetics is temperature sensitive, which can be used for temperature measurements. For measurements using a TCSPC fluorimeter with a time resolution of ~ 100 ps, the most promising temperature range is 260–290 K, where the average fluorescence decay time of ThT in glycerol varies from 2.0 to 0.5 ns (Fig. 5, *b*).

Similar properties are also observed for the fluorescence kinetics of the 6-Me-BTA-2C cation in 99%-glycerol: non-monoexponentiality (Table 3, 4), an increase in the average attenuation time (τ) with increasing wavelength of the emission spectrum (Fig. 6, *c, d*). The long-lived component with $\tau \sim 3.4$ ns at the short-wavelength edge of the 6-Me-BTA-2C fluorescence spectrum at 440 and 450 nm (Table 3)

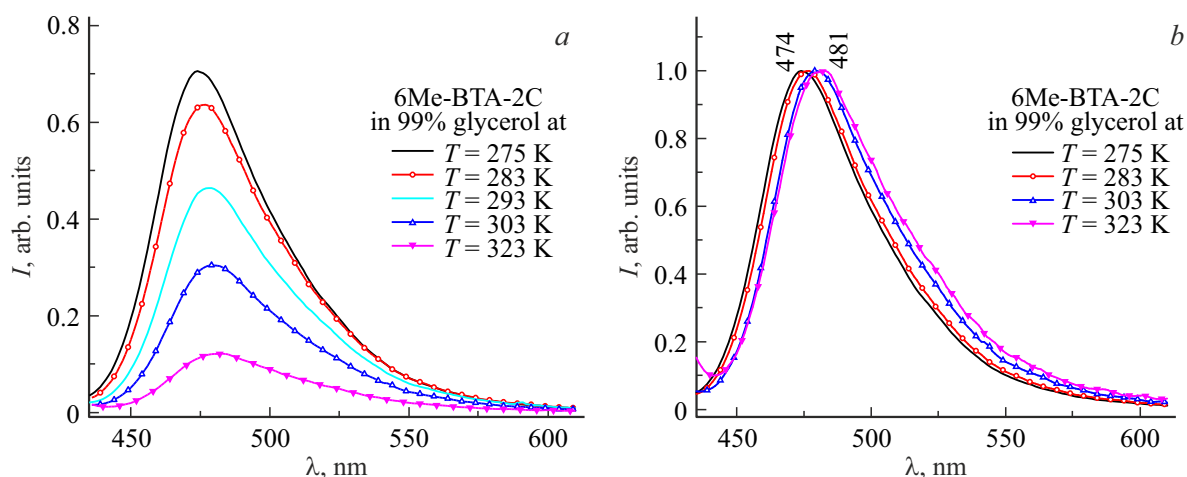


Figure 4. Initial (a) and normalized (b) fluorescence spectra of 6-Me-BTA-2C in 99%-glycerol at various temperatures. $\lambda_{exc} = 415$ nm.

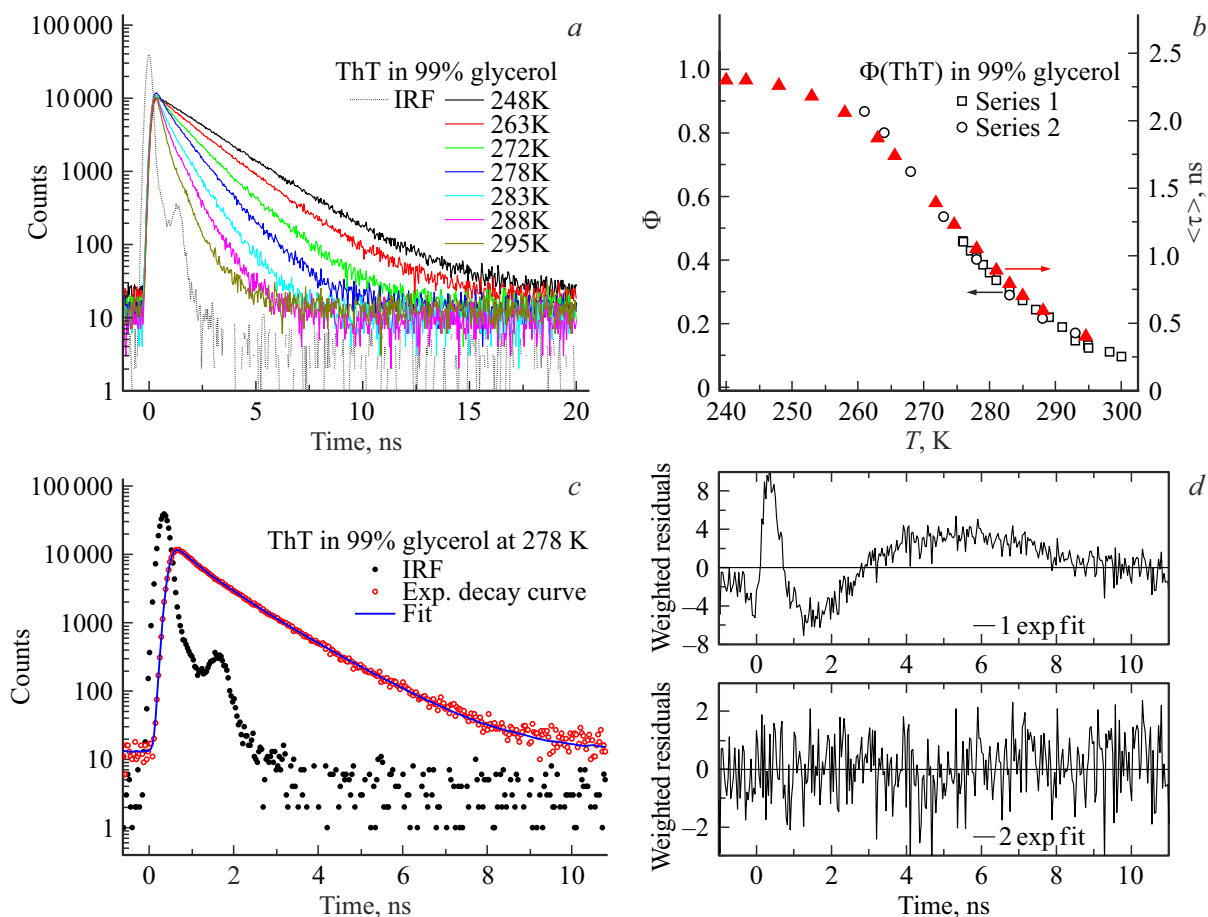


Figure 5. (a) Fluorescence decay kinetics of ThT in 99%-glycerol at various temperatures; $\lambda_{exc} = 407$ nm, $\lambda_{em} = 480$ nm; the dotted curve indicates instrument response function IRF. (b) Temperature dependences of quantum yield Φ and mean lifetime $\langle \tau \rangle$ of ThT fluorescence in glycerol. (c) Fluorescence decay kinetics of ThT in 99%-glycerol at $T = 278$ K; filled circles — instrument response function IRF, hollow circles — experimental kinetics curve, solid curve — fitting by multiexponential model. (d) Plots of weighted residuals between experimental and calculated curves of ThT emission decay in 99%-glycerol at $T = 278$ K for mono and biexponential fits.

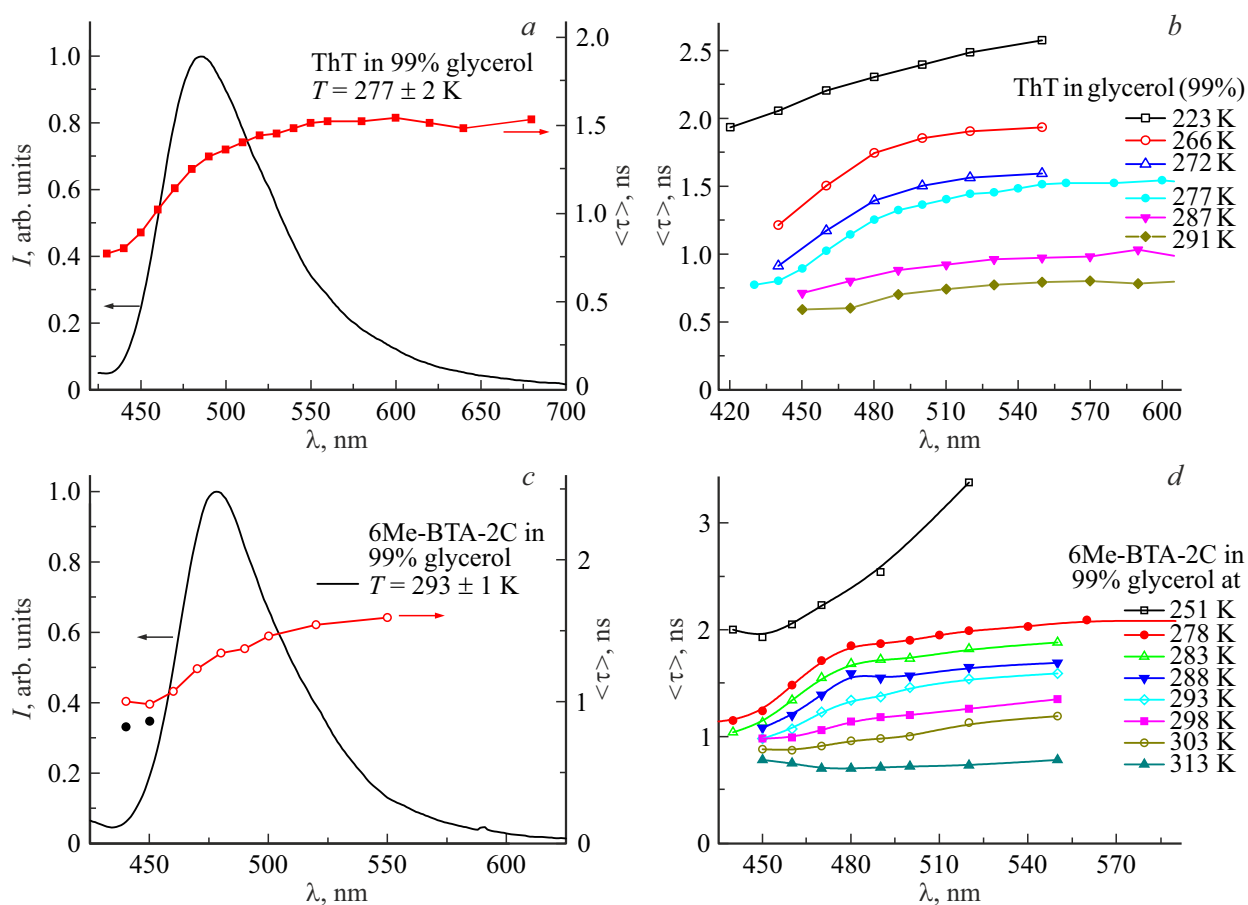


Figure 6. Average decay lifetime (τ) versus fluorescence wavelength for ThT (a,b) and 6-Me-BTA-2C (c,d) in 99%-glycerol at various temperatures. (a) Fluorescence spectrum for ThT in glycerol and dependence $\langle\tau\rangle$ on λ at 277 K. (b) Dependence $\langle\tau\rangle$ on the fluorescence wavelength of ThT for temperatures from 223 to 291 K. (c) Fluorescence spectrum of 6-Me-BTA-2C in glycerol and dependence $\langle\tau\rangle$ on the spectrum at 293 K. (d) Dependence $\langle\tau\rangle$ on the wavelength of 6-Me-BTA-2C fluorescence for temperatures from 251 to 313 K.

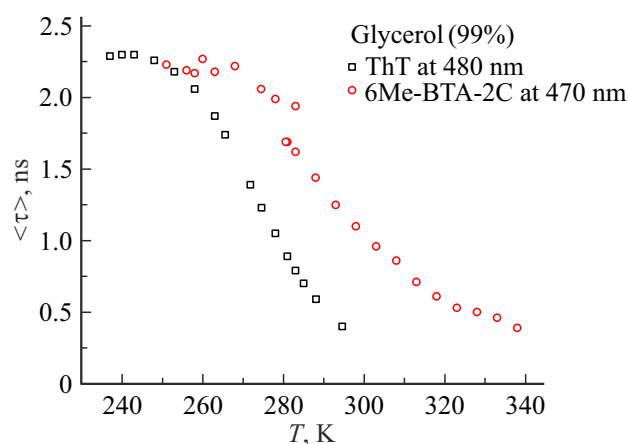


Figure 7. Average fluorescence decay lifetime (τ) for ThT and 6-Me-BTA-2C in 99%-glycerol as a function of temperature. $\lambda_{\text{exc}} = 407 \text{ nm}$, $\lambda_{\text{em}} = 480 \text{ nm}$ (ThT) and 470 nm (6-Me-BTA-2C).

is most likely due to the presence of a small amount of the neutral form of molecule 6-Me-BTA-2 [42] in the sample. In Fig. 6,c the black circles mark the average

attenuation time (τ) for 6-Me-BTA-2C, if the contribution of the long-lived component with $\tau \sim 3.4 \text{ ns}$ is excluded from the calculation. The presence of this impurity also causes an anomalous rise in the $\langle\tau\rangle$ value at the short-wavelength edge of the fluorescence spectrum (Fig. 6,d), especially for the dye at higher temperatures.

Despite the similarity of ThT and 6Me-BTA-2C molecules (Fig. 1), changes in the FMR structure, associated with change of a substituent at the nitrogen atom of the benzothiazole ring from a methyl group to hydrogen, lead to a significant decrease in the effective rate constant of the TICT reaction for 6-Me-BTA-2C. In this case, the temperature-sensitive region for the fluorescence of this dye in glycerol shifts towards higher temperatures (Fig. 7).

Thus, temperature measurements based on the fluorescence decay kinetics of ThT and 6-Me-BTA-2C in glycerol are possible starting from 260 K (for ThT) and 280 K (for 6-Me-BTA-2C). The upper limit of the temperature range is determined by the time resolution of the spectrometer, and when measured by the TCSPC method with resolution of $\sim 100 \text{ ps}$, the temperature range available for measurements

Table 2. Parameters of ThT fluorescence decay kinetics in 99%-glycerol at different wavelengths for $T = (277 \pm 1.5)$ K, $\lambda_{\text{exc}} = 407$ nm

λ	α_1	τ_1 , ns	S_1 , %	α_2	τ_2 , ns	S_2 , %	α_3	τ_3 , ns	S_3 , %	$\langle \tau \rangle$, ns*	χ^2
430	0.780	0.29	47.3	0.220	1.15	52.7				0.75 ± 0.06	1.32
	0.652	0.22	31.6	0.284	0.72	45.4	0.064	1.62	23.1	0.77 ± 0.07	1.07
440	0.761	0.36	49.4	0.239	1.18	50.6				0.78 ± 0.06	1.68
	0.636	0.29	34.4	0.330	0.87	53.1	0.035	1.94	12.6	0.80 ± 0.07	1.37
460	0.677	0.57	46.2	0.323	1.40	53.8				1.02 ± 0.06	1.16
	0.514	0.50	31.0	0.311	0.96	35.8	0.176	1.58	33.2	1.02 ± 0.06	1.16
480				0.606	0.80	43.9	0.394	1.58	56.1	1.24 ± 0.06	1.19
	-0.225	0.13	-2.8	0.542	0.68	35.9	0.458	1.50	66.9	1.25 ± 0.06	1.06
500				0.595	0.98	46.2	0.405	1.67	53.8	1.35 ± 0.06	1.27
	-0.335	0.11	-3.3	0.451	0.76	29.7	0.549	1.55	73.5	1.36 ± 0.06	1.01
520				0.883	1.24	81.0	0.117	2.20	19.0	1.42 ± 0.06	1.58
	-0.402	0.12	-3.9	0.608	1.00	49.1	0.392	1.73	54.9	1.44 ± 0.06	1.16
540	-0.393	0.16	-4.8	0.505	0.97	38.9	0.495	1.68	65.9	1.48 ± 0.06	1.06
560	-0.473	0.14	-5.0	0.811	1.20	75.0	0.189	2.07	30.0	1.52 ± 0.06	1.16
580	-0.445	0.16	-5.3	0.634	1.13	54.8	0.366	1.80	50.5	1.52 ± 0.06	1.02
600	-0.552	0.16	-6.8	0.637	1.10	55.1	0.363	1.82	51.7	1.54 ± 0.06	1.13
620	-0.583	0.18	-8.8	0.429	0.84	30.4	0.571	1.62	78.4	1.51 ± 0.06	0.97
640	-0.776	0.09	-5.5	1.000	1.41	105.5				1.48 ± 0.06	1.47
	-0.488	0.19	-8.1	0.380	0.79	25.4	0.620	1.57	82.7	1.48 ± 0.06	1.12
680	-1.217	0.09	-8.8	1.000	1.36	108.8				1.47 ± 0.06	1.20
	-1.217	0.13	-14.1	0.484	0.91	39.6	0.516	1.60	74.5	1.53 ± 0.07	1.06

Note. * Estimated standard deviation for $\langle \tau \rangle$ is stated.

is 260–290 K (ThT in glycerol) and 280–320 K (6-Me-BTA-2C in glycerol).

Conclusions

The quantum yield and fluorescence kinetics of ThT benzothiazol-aniline derivatives exhibiting FMR properties are temperature-sensitive, which allows these compounds to be used as temperature sensors.

It has been experimentally shown that the TICT reaction of intramolecular charge transfer accompanied by conformational changes is the dominant process of non-radiative deactivation of the ThT excited state in glycerol up to temperatures of $T \sim 260$ K. The effective rate constant of the TICT reaction is determined by the viscous properties of the microenvironment, and changing the temperature of the glycerol solution from 261 to 353 K leads to an increase in its value by a ~ 3 orders of magnitude. Based on the data on the quantum yield and fluorescence kinetics of ThT in 99%-glycerol, the constant of the radiative

transition from the excited LE state $k_r \approx 0.4 \cdot 10^9 \text{ s}^{-1}$ was determined.

The fluorescence kinetics of the considered dyes in glycerol has a non-monoexponential character, depends on the fluorescence detection wavelength, and its description requires the use of at least 2 exponential components. The non-monoexponentiality of the kinetics is associated with heterogeneity of the microenvironment of FMR molecules in glycerol, as well as with occurrence of a spectral relaxation process in the excited state of dyes, the characteristic time of which is close in value of the lifetime of the excited LE state responsible for the FMR fluorescence. The process of spectral relaxation manifests itself both in stationary fluorescence spectra (spectra shift depending on temperature) and in kinetics (a monotonic increase in the mean lifetime $\langle \tau \rangle$ with an increase in the fluorescence detection wavelength and the appearance of components with a negative amplitude on the red edge of the spectrum).

Table 3. Parameters of 6Me-BTA-2C fluorescence decay kinetics in 99%-glycerol at temperature (288 ± 1) K, $\lambda_{\text{exc}} = 407$ nm

λ	α_1	τ_1 , ns	S_1 , %	α_2	τ_2 , ns	S_2 , %	α_3	τ_3 , ns	S_3 , %	$\langle\tau\rangle$, ns*	χ^2
440	0.702	0.37	38.8	0.298	1.39	61.2				1.00 ± 0.06	1.55
	0.635	0.32	30.4	0.352	1.18	62.9	0.013	3.40	6.7	1.06 ± 0.10	1.16
450	0.719	0.56	48.7	0.281	1.51	51.3				1.05 ± 0.06	1.27
	0.650	0.51	40.8	0.341	1.34	55.7	0.009	3.40	3.6	1.08 ± 0.10	1.20
460				0.623	0.76	44.9	0.377	1.55	55.1	1.19 ± 0.06	1.48
	-0.381	0.16	-7.2	0.563	0.54	35.1	0.437	1.43	72.2	1.20 ± 0.07	1.12
470	-0.444	0.16	-6.1	0.551	0.94	44.4	0.449	1.60	61.7	1.39 ± 0.07	1.05
480	-1.152	0.12	-11.1	1.000	1.43	111.1				1.57 ± 0.06	1.36
	-1.164	0.13	-12.6	0.842	1.31	89.0	0.158	1.86	23.6	1.59 ± 0.07	1.19
490	-0.566	0.16	-6.7	1.000	1.45	106.7				1.54 ± 0.06	1.18
	-0.536	0.20	-8.1	0.569	1.22	53.1	0.431	1.66	55.0	1.55 ± 0.06	1.05
500	-0.593	0.16	-7.1	1.000	1.46	107.1				1.56 ± 0.06	1.24
	-0.563	0.18	-7.8	0.953	1.40	99.8	0.047	2.29	8.0	1.57 ± 0.07	1.15
520	-0.639	0.21	-9.9	1.000	1.50	109.9				1.63 ± 0.06	1.12
	-0.622	0.23	-10.8	0.987	1.46	107.5	0.013	3.24	3.3	1.65 ± 0.10	1.03
550	-0.666	0.22	-10.6	1.000	1.55	110.6				1.69 ± 0.06	1.07

Note. * Estimated standard deviation for $\langle\tau\rangle$ is stated.

Table 4. Parameters of 6Me-BTA-2C fluorescence decay kinetics in 99%-glycerol at 470 nm at different temperatures, $\lambda_{\text{exc}} = 407$ nm

λ	α_1	τ_1 , ns	S_1 , %	α_2	τ_2 , ns	S_2 , %	α_3	τ_3 , ns	S_3 , %	$\langle\tau\rangle$, ns*	χ^2
283	-0.555	0.14	-5.6	0.803	1.35	77.0	0.197	2.05	28.7	1.62 ± 0.07	1.05
293	-0.412	0.14	-5.8	0.469	0.71	32.8	0.531	1.40	73.1	1.25 ± 0.07	1.13
303				0.884	0.77	79.0	0.116	1.57	21.0	0.94 ± 0.06	1.27
	-0.596	0.06	-4.8	0.813	0.71	72.3	0.187	1.39	32.5	0.96 ± 0.07	1.17
313				0.936	0.55	83.8	0.064	1.54	16.2	0.71 ± 0.06	1.50
	-0.400	0.04	-2.9	0.929	0.54	85.1	0.071	1.48	17.8	0.72 ± 0.08	1.49
323				0.949	0.37	83.7	0.051	1.35	16.3	0.53 ± 0.06	1.25
333				0.957	0.28	82.5	0.043	1.31	17.5	0.46 ± 0.06	1.21
343				0.968	0.20	83.8	0.032	1.18	16.2	0.36 ± 0.06	1.30

Note. * Estimated standard deviation for $\langle\tau\rangle$ is stated.

It has been found that temperature measurements based on the fluorescence decay kinetics are possible for ThT in glycerol solutions starting from 260 K, and for 6-Me-BTA-2C in glycerol — starting from 280 K. The upper limit of the temperature range available for measurements is determined by the time resolution of the spectrometer, and at the time resolution of ~ 100 ps it corresponds to 290 and 320 K for ThT and 6-Me-BTA-2C glycerol solutions, respectively.

The data obtained can be used to develop fluorescent sensors for nanothermometry, to visualize temperature gradients with high spatial resolution using fluorescence microscopy.

Funding

The work was supported by the Ministry of Education of the Republic of Belarus (project 3.04 of the „Convergence-

2020⁶ program and project 3.01.3.3 of the „Convergence-2025“ program).

Conflict of interest

The authors declare that they have no conflict of interest.

References

- [1] J. Zhou, B. del Rosal, D. Jaque, S. Uchiyama, D. Jin. *Nature Methods*, **17** (10), 967 (2020). DOI: 10.1038/s41592-020-0957-y
- [2] D. Jaque, F. Vetrone. *Nanoscale*, **4** (15), 4301 (2012). DOI: 10.1039/C2NR30764B
- [3] B. del Rosal, E. Ximendes, U. Rocha, D. Jaque. *Advanced Optical Materials*, **5** (1), 1600508 (2017). DOI: 10.1002/adom.201600508
- [4] K. Grattan, A. Palmer. *Review of Scientific Instruments*, **56** (9), 1784 (1985). DOI: 10.1063/1.1138094
- [5] S. Collins, G. Baxter, S. Wade, T. Sun, K. Grattan, Z. Zhang, A. Palmer. *J. Appl. Phys.*, **84** (9), 4649 (1998). DOI: 10.1063/1.368705
- [6] J. Feng, K. Tian, D. Hu, S. Wang, S. Li, Y. Zeng, Y. Li, G. Yang. *Angewandte Chemie International Edition*, **50** (35), 8072 (2011). DOI: 10.1002/ange.201102390
- [7] X. Liu, S. Li, J. Feng, Y. Li, G. Yang. *Chem. Commun.*, **50** (21), 2778 (2014). DOI: 10.1039/C3CC49147A
- [8] A. Bednarkiewicz, L. Marciniak, L.D. Carlos, D. Jaque. *Nanoscale*, **12** (27), 14405 (2020). DOI: 10.1039/D0NR03568H
- [9] B.M. Uzhinov, V.L. Ivanov, M.Ya. Melnikov. *Uspekhi khimii*, **80** (12), 1231 (2011) (in Russian).
- [10] M.A. Haidekker, E.A. Theodorakis. *Org. Biomol. Chem.*, **5** (11), 1669 (2007). DOI: 10.1039/b618415d
- [11] M.A. Haidekker, E.A. Theodorakis. *J. Biological Engineering*, **4** (1), 11 (2010). DOI: 10.1186/1754-1611-4-11
- [12] E. Voropai, M. Samtsov, K. Kaplevskii, A. Maskevich, V. Stepuro, O. Povarova, I. Kuznetsova, K. Turoverov, A. Fink, V. Uverskii. *J. Appl. Spectrosc.*, **70** (6), 868 (2003). DOI: 10.1023/B:JAPS.0000016303.37573.7e
- [13] V.I. Stsiapura, A.A. Maskevich, V.A. Kuzmitsky, V.N. Uversky, I.M. Kuznetsova, K.K. Turoverov. *J. Phys. Chem. B*, **112** (49), 15893 (2008). DOI: 10.1021/jp805822c
- [14] V.I. Stsiapura, S.A. Kurhuzenkau, V.A. Kuzmitsky, O.V. Boganov, S.A. Tikhomirov. *J. Phys. Chem. A*, **120** (28), 5481 (2016). DOI: 10.1021/acs.jpca.6b02577
- [15] M.J. van der Meer, H. Zhang, M. Glasbeek. *J. Chem. Phys.*, **112** (6), 2878 (2000). DOI: 10.1063/1.480929
- [16] M. Glasbeek, H. Zhang, P. Changelnet, P. Plaza, M.M. Martin, W. Rettig. *Femtochemistry: With the Nobel Lecture of A Zewail*, 417 (2001). DOI: 10.1002/3527600183.ch26
- [17] Y. Erez, N. Amdursky, R. Gepshtein, D. Huppert. *J. Phys. Chem. A*, **116** (49), 12056 (2012). DOI: 10.1021/jp309471w
- [18] D. Ben-Amotz, C. Harris. *J. Chem. Phys.*, **86** (9), 4856 (1987). DOI: 10.1063/1.452656
- [19] A. Mokhtari, L. Fini, J. Chesnoy. *J. Chem. Phys.*, **87** (6), 3429 (1987). DOI: 10.1063/1.452987
- [20] R.O. Loutfy, B.A. Arnold. *J. Phys. Chem.*, **86** (21), 4205 (1982). DOI: 10.1021/j100218a023
- [21] R.O. Loutfy, K.Y. Law. *J. Phys. Chem.*, **84** (21), 2803 (1980). DOI: 10.1021/j100458a027
- [22] T.T. Vu, R. Méallet-Renault, G. Clavier, B.A. Trofimov, M.K. Kuimova. *J. Mater. Chem. C*, **4** (14), 2828 (2016). DOI: 10.1039/C5TC02954F
- [23] E. Bahaidarah, A. Harriman, P. Stachelek, S. Rihn, E. Heyer, R. Ziessel. *Photochemical & Photobiological Sciences*, **13** (10), 1397 (2014). DOI: 10.1039/C4PP00204K
- [24] A. Vyšniauskas, I. López-Duarte, N. Duchemin, T.-T. Vu, Y. Wu, E.M. Budynina, Y.A. Volkova, E.P. Cabrera, D.E. Ramírez-Ornelas, M.K. Kuimova. *Phys. Chem. Chem. Phys.*, **19** (37), 25252 (2017). DOI: 10.1039/C7CP03571C
- [25] A. Vyšniauskas, D. Ding, M. Qurashi, I. Boczarow, M. Balaz, H.L. Anderson, M.K. Kuimova. *Chemistry-A European J.*, **23** (46), 11001 (2017). DOI: 10.1002/chem.201700740
- [26] Y.-J. Jin, R. Dogra, I.W. Cheong, G. Kwak. *ACS Appl. Mater. & Interfaces*, **7** (26), 14485 (2015). DOI: 10.1021/acsami.5b03842
- [27] A.A. Maskevich, V.I. Stsiapura, V.A. Kuzmitsky, I.M. Kuznetsova, O.I. Povarova, V.N. Uversky, K.K. Turoverov. *J. Proteome Research*, **6** (4), 1392 (2007). DOI: 10.1021/pr0605567
- [28] N. Amdursky, Y. Erez, D. Huppert. *Accounts of Chemical Research*, **45** (9), 1548 (2012). DOI: 10.1021/ar300053p
- [29] V.I. Stsiapura, A.A. Maskevich, V.A. Kuzmitsky, K.K. Turoverov, I.M. Kuznetsova. *J. Phys. Chem. A*, **111** (22), 4829 (2007). DOI: 10.1021/jp070590o
- [30] V.I. Stsiapura. *J. Computational Chem.*, **41** (21), 1874 (2020). DOI: 10.1002/jcc.26358
- [31] V.I. Stsiapura, A.A. Maskevich, S.A. Tikhomirov, O.V. Baganov. *J. Phys. Chem. A*, **114** (32), 8345 (2010). DOI: 10.1021/jp105186z
- [32] A.T.R. Williams, S.A. Winfield, J.N. Miller. *Analyst*, **108** (1290), 1067 (1983). DOI: 10.1039/AN9830801067
- [33] C. Yaws. *Chemical Properties Handbook*. (McGraw-Hill Education, 1999).
- [34] J.A. Trejo González, M.P. Longinotti, H.R. Corti. *J. Chemical & Engineering Data*, **56** (4), 1397 (2011). DOI: 10.1021/je101164q
- [35] A. Maskevich, V. Stepuro, S. Kurguzenkov, A. Lavysch. *Vesnik Grodzenskaga dzyarzhauņa universiteta imya Yanki Kupaly Seryya 2 Matematyka Fizika Infarmatyka, vylichalnaya tekhnika i kiravanne*, **3** (159), 107 (2013) (in Belorussian).
- [36] D.V. O'Connor, D. Phillips. *Time-correlated Single Photon Counting*. (Academic Press, New York., 1984).
- [37] V. Stepuro. *Vesnik Grodzenskaga dzyarzhauņa universiteta imya Yanki Kupaly Seryya 2*, **5** (1), 52 (2001) (in Belorussian).
- [38] R. Lampert, S. Meech, J. Metcalfe, D. Phillips, A. Schaap. *Chem. Phys. Lett.*, **94** (2), 137 (1983). DOI: 10.1016/0009-2614(83)87560-5
- [39] D. Toptygin. *J. Fluorescence*, **13** (3), 201 (2003). DOI: 10.1023/A:1025033731377
- [40] H. El-Kashef. *Physica B: Condensed Matter*, **311** (3–4), 376 (2002). DOI: 10.1016/S0921-4526(01)00642-1
- [41] A. Chakraborty, D. Seth, P. Setua, N. Sarkar. *J. Phys. Chem. B*, **110** (11), 5359 (2006). DOI: 10.1021/jp056650c
- [42] S.D. Gogoleva, E.V. Kalganova, A.A. Maskevich, A.A. Lugovskii, V.A. Kuzmitsky, M. Goswami, O.V. Baganov, S.A. Tikhomirov, V.I. Stsiapura. *J. Photochemistry and Photobiology A: Chemistry*, **358**, 76 (2018). DOI: <https://doi.org/10.1016/j.jphotochem.2018.03.003>